

## Crystal Structure of the Host Lattices of the Superconductors $\text{Li}_x\text{MNX}$ ( $\text{M} = \text{Zr}, \text{Hf}$ ; $\text{X} = \text{Cl}, \text{Br}$ )

Amparo Fuertes,\* Mikhail Vlassov,<sup>†</sup>  
Daniel Beltrán-Porter,<sup>‡</sup> Pere Alemany,<sup>§</sup>  
Enric Canadell, Nieves Casañ-Pastor, and  
M. Rosa Palacín

*Institut de Ciència de Materials de Barcelona (C.S.I.C.), Campus U.A.B., 08193 Bellaterra, Spain, Institut de Ciència de Materials de la Universitat de València, C/Dr. Moliner 50, Edificio de Investigación, 46100 Burjassot, Spain, and Departament de Química-Física, Facultat de Química, Universitat de Barcelona, Diagonal 647, 08028 Barcelona, Spain*

Received October 13, 1998

Revised Manuscript Received November 25, 1998

The recent discovery of superconductivity in lithium-doped  $\beta\text{-MnCl}$ <sup>1,2</sup> ( $\text{M} = \text{Hf}, \text{Zr}$ ) at temperatures higher than that shown by intermetallic  $\text{Nb}_3\text{Ge}$  has opened novel perspectives in the search of new covalent non-oxide layered superconductors. The crystal and electronic structures of the undoped materials, and those of the intercalated superconductors, have been described<sup>1,2,4</sup> on the basis of the model reported by Juza et al.<sup>5</sup> as  $\text{CdCl}_2$  and  $\text{CdI}_2$  structural types (or as a random distribution of layers of both types),<sup>6</sup> in a cell of dimensions  $a = 3.6 \text{ \AA}$  and  $c = 9.2 \text{ \AA}$  with the space group  $P\bar{3}m1$ . (See Figure 1a) In this model, there are two individual sheets  $[\text{M}-\text{N}]$  occupying the Cd positions that are sandwiched between the close-packed chloride or iodide layers. When we became interested on these compounds, we soon realized that this description was not appropriate since attempts to refine new powder X-ray diffraction data for  $\beta\text{-ZrNCl}$ ,  $\beta\text{-ZrNBr}$ , and  $\beta\text{-HfNCl}$  using the atomic positions from Juza's model were systematically unsuccessful. The determination of the correct structure of the host lattice of this new family of superconductors is not only a matter of academic interest but also an essential step in any attempt to find correlations between  $T_c$  and the structural or electronic aspects of these phases. In this paper we report the crystal structure for  $\beta\text{-HfNCl}$ ,  $\beta\text{-ZrNCl}$ , and  $\beta\text{-ZrNBr}$  from powder X-ray and electron diffraction data, as well as electronic band structure calculations based on the new structural model. The most remarkable difference with the structure proposed by Juza et al. lies in the

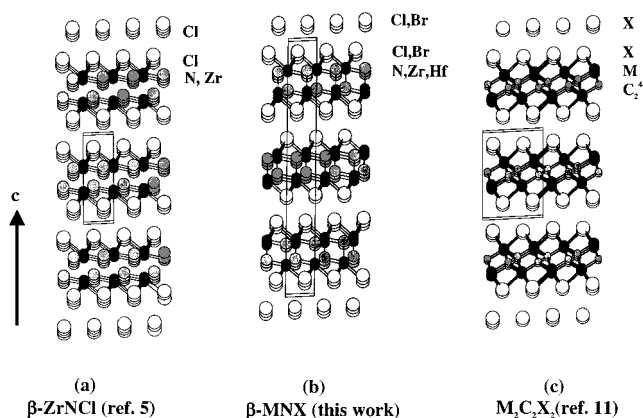


**Figure 1.** Perspective view of the structures of (a)  $\beta\text{-ZrNCl}$  (ref 5), (b)  $\beta\text{-ZrNCl}$ ,  $\beta\text{-ZrNBr}$  and  $\beta\text{-HfNCl}$  (this work), and (c)  $\text{M}_2\text{C}_2\text{X}_2$  ( $\text{M} = \text{rare earth}$ ,  $\text{X} = \text{halide}$ ) (ref 11). Black spheres correspond to metal atoms; white and gray spheres represent halide and carbon or nitrogen atoms, respectively.

packing of the two layers  $\text{X}-\text{M}-\text{N}$  forming the double sheet  $[\text{X}-\text{M}-\text{N}-\text{N}-\text{M}-\text{X}]$ . These layers are shifted perpendicularly to the  $c$  axis with respect to the above model, implying the existence of an additional  $\text{M}-\text{N}$  bond joining the layers. (Figure 1b) The band structure calculations show that the lowest empty levels of the host structure (i.e., those filled with electrons in the lithiated phases) are completely different when the electronic structure is based on the model of Juza et al.<sup>5</sup> or on our new structure. We also report superconductivity for the first time at 13.5 K in lithium-doped  $\beta\text{-ZrNBr}$ .<sup>7</sup>

Figure 2 shows the observed and calculated X-ray diffraction patterns for  $\beta\text{-ZrNBr}$ ,  $\beta\text{-ZrNCl}$ , and  $\beta\text{-HfNCl}$ , and Figure 3 shows representative electron diffraction patterns along  $[001]$  and  $[100]$  zone axes for the three compounds. Indexation of the reflections in these planes (and in others obtained by tilting the crystals around the  $[001]$  axis) leads to a hexagonal cell with parameters  $a \cong 3.6 \text{ \AA}$ ,  $c \cong 27.7 \text{ \AA}$  (for  $\text{X} = \text{Cl}$ ) and  $29.3 \text{ \AA}$  (for  $\text{X} = \text{Br}$ ). The observed reflection conditions ( $hkl$ ,  $-h + k + l = 3n$ ;  $h\bar{h}l$ ,  $h + l = 3n$ ;  $hhl$ ,  $l = 3n$ , and  $00l$ ,  $l = 3n$ ) are

(7) The syntheses of  $\beta\text{-HfNCl}$ ,  $\beta\text{-ZrNCl}$ , and  $\beta\text{-ZrNBr}$  were carried out by the reaction of Hf or Zr metals (Aldrich 99.5%) with  $\text{NH}_4\text{Cl}$  or  $\text{NH}_4\text{Br}$  (Aldrich 99.99%) at  $850 \text{ }^\circ\text{C}$ , followed by transport purification under a temperature gradient in an evacuated quartz tube. Chemical lithiation reactions were done between room temperature and  $50 \text{ }^\circ\text{C}$  by dispersion of the powders in a 0.1 M solution of *n*-butyllithium in hexane, using evacuated Ar sealed glass tubes. Electrochemical tests were made on powder samples with Swagelok two-electrode cells using lithium foil as counter electrode and 1 M  $\text{LiPF}_6$  in 1:1 EC/DMC (ethylene carbonate/dimethyl carbonate) as electrolyte. Handling of lithiated samples and cell preparation was done in an Ar-filled glovebox. Electron diffraction patterns and XEDS analyses were obtained in a JEOL 1210 transmission electron microscope operating at 120 kV. Lithium contents were determined by atomic emission analysis. X-ray diffraction patterns were taken in a Seifert X-ray diffractometer using  $\text{Cu K}\alpha$  radiation. The structures were solved by Rietveld analysis of the X-ray diffraction pattern profiles with the Fullprof program.<sup>8</sup> The profile fitting of the data was performed with a pseudo-Voigt function, including asymmetry and preferred orientation corrections (14 profile, 7 global, and 8 intensity-dependent refined parameters in the case of  $\text{ZrNBr}$ ); the background was refined to a 5th degree polynomial. Magnetic susceptibility measurements were performed in a Quantum Design SQUID magnetometer, on powder samples double sealed under Ar atmosphere, under zero-field-cooled and field-cooled conditions ( $H_{\text{measured}} = 30 \text{ G}$ ).

<sup>†</sup> Permanent address: Earthcrust Research Institute, St. Petersburg University, Russia.

<sup>‡</sup> Institut de Ciència de Materials de la Universitat de València.

<sup>§</sup> Universitat de Barcelona.

(1) Yamanaka, S.; Hohetama, K.; Kawaji, H. *Nature* **1998**, *392*, 580–582.

(2) a) Yamanaka, S.; Kawaji, H.; Hotehama, K.; Ohashi, M. *Adv. Mater.* **1996**, *8*, 771–774. (b) Kawaji, H.; Hotehama, K.; Yamanaka, S. *Chem. Mat.* **1997**, *9*, 2127–2130.

(3) Gavaler, J. R. *Appl. Phys. Lett.* **1973**, *23*, 480–482.

(4) Woodward, P. M.; Vogt, T. *J. Solid State Chem.* **1998**, *138*, 207–219.

(5) Juza, R.; Friedrichsen, H. *Z. Anorg. Allg. Chem.* **1964**, *332*, 173–178.

(6) Ohashi, M.; Yamanaka, S.; Sumihara, M.; Hattori, M. *J. Solid State Chem.* **1988**, *75*, 99–104.

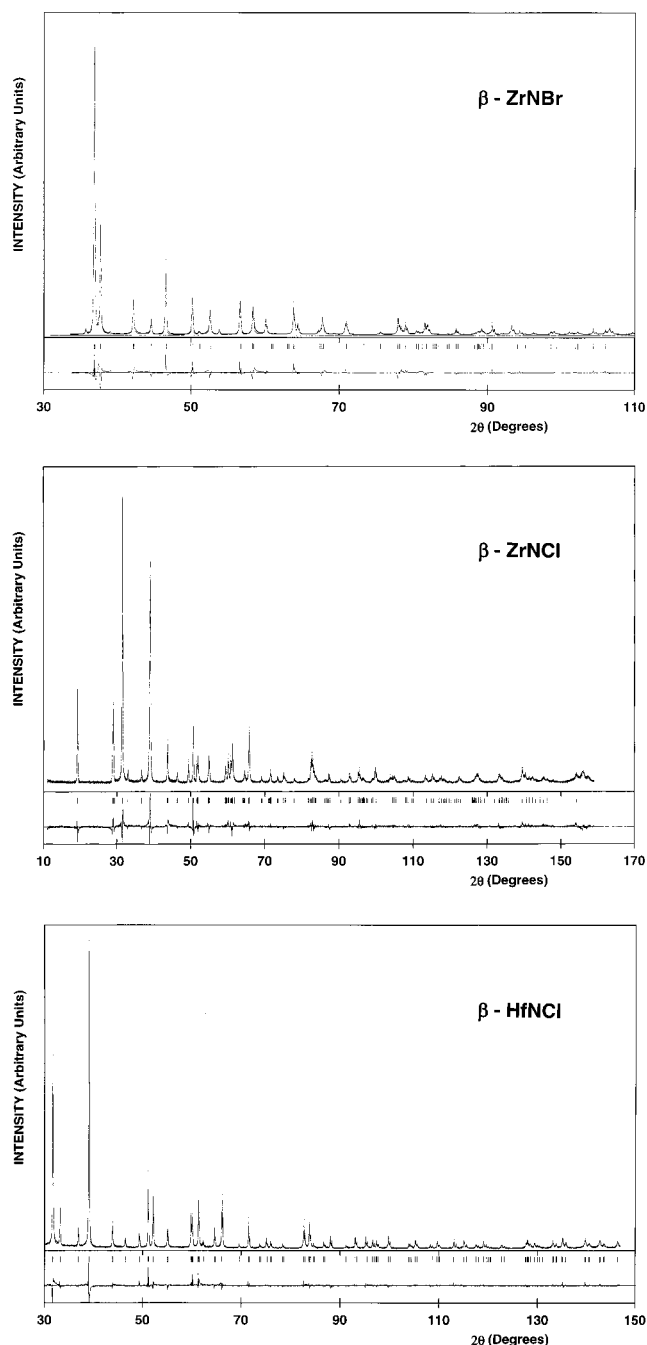


**Figure 2.** Observed and calculated X-ray diffraction patterns for  $\beta$ -ZrNBr,  $\beta$ -ZrNCl, and  $\beta$ -HfNCl.

consistent with the space groups  $R\bar{3}$ ,  $R\bar{3}2$ ,  $R\bar{3}m$ , and  $R\bar{3}m$ . Diffuse lines are observed along the directions parallel to  $c^*$ , indicating disorder in the stacking of the planes perpendicular to this axis. Table 1 summarizes the results of the Rietveld refinements for the three compounds in the space group  $R\bar{3}m$ , and Figure 1b shows a perspective view of the structure. The observation of broad X-ray diffraction peaks connecting  $hkl$  reflections with the same  $h+k$  (in contrast to sharp  $00l$  and  $lll$  peaks) confirm some disorder along  $c$  and account for difficulties in defining the profile function.

(8) Rodríguez-Carvajal, J. Program FULLPROF, Version 2.5, April 1994, ILL, unpublished.

(9) Hulliger, F. *Structural Chemistry of Layer-Type Phases*; Lévy, F., Ed.; D. Reidel Publishing Company: Dordrecht/Boston, 1976; Vol. 5, p 263.

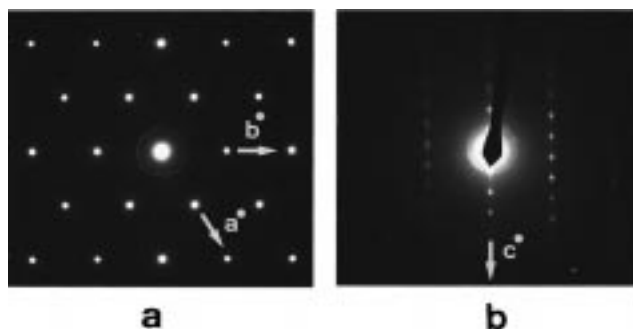


**Figure 3.** Representative electron diffraction patterns along the (a) [001] and (b) [100] zone axes for  $\beta$ -MNX (M = Hf, Zr; X = Cl, Br).

**Table 1. Crystallographic Parameters for  $\beta$ -HfNCl,  $\beta$ -ZrNCl, and  $\beta$ -ZrNBr (Space Group  $R\bar{3}m$ ,  $Z = 6$ , All Atoms in Wyckoff Site 6C)**

parameter	$\beta$ -HfNCl	$\beta$ -ZrNCl	$\beta$ -ZrNBr
$a$ (Å)	3.5744(3)	3.6031(6)	3.6379(5)
$c$ (Å)	27.7075(9)	27.672(2)	29.263(2)
M (Zr or Hf)			
$z/c$	0.1194(1)	0.1192(1)	0.1222(1)
$B_{iso}$ (Å <sup>2</sup> )	0.28(2)	0.47(3)	0.7(2)
$\beta_{11} \times 10^3$	18(1)	30(2)	26(3)
$\beta_{33} \times 10^3$ <sup>c</sup>	0	0	0
$\beta_{12} \times 10^3$	9(1)	16(2)	13(3)
X (Cl or Br)			
$z/c$	0.3887(4)	0.3878(2)	0.3885(1)
$B_{iso}$ (Å <sup>2</sup> )	0.6(1)	0.72(6)	1.1(2)
$\beta_{11} \times 10^3$	32(5)	48(4)	40(4)
$\beta_{33} \times 10^3$ <sup>c</sup>	0	0	0
$\beta_{12} \times 10^3$	16(5)	24(4)	20(4)
N			
$z/c$	0.199(2)	0.200(1)	0.202(1)
$B_{iso}$ (Å <sup>2</sup> ) <sup>c</sup>	0.8(3)	2.4 (2)	0.5(2)
$N_p, N_{refl}, N_{indep}$ <sup>d</sup>	5825, 216, 106	6672, 232, 112	6290, 245, 121
$P_p, P_i, P_g$ <sup>e</sup>	12, 8, 7	12, 8, 7	12, 8, 7
$R_{Bragg}, R_F, \chi^2$	7.9, 5.1, 2.6	8.1, 5.2, 2.2	8.4, 6.1, 11.7
$R_p, R_{wp}, R_{exp}$ <sup>a</sup>	21.5, 13.5, 21.6	21.0, 24.7, 16.7	21.1, 25.1, 8.7
$f_p$ <sup>b</sup>	3.3	3.5	3.4
$d(M-N)$ (Å)	2.20(6)	2.17(3)	2.30(4)
	2.11(1) $\times$ 3	2.125(6) $\times$ 3	2.121(6) $\times$ 3
$d(M-X)$ (Å)	2.722(7) $\times$ 3	2.755(4) $\times$ 3	2.873(4) $\times$ 3

<sup>a</sup> Conventional Rietveld  $R$  factors ( $R_p, R_{exp}$ ) are calculated by using background corrected counts. <sup>b</sup> Standard deviations in the table are multiplied by the Pawley parameter  $f_p$  (to get realistic values) (see ref 8). <sup>c</sup>  $\beta_{33}$  values were restricted to be zero because of the very small and negative values resulting from the refinement. N atom thermal vibrations were restricted to be isotropic. <sup>d</sup>  $N_p, N_{refl}, N_{indep}$  refer to the number of experimental points, total reflections, and independent reflections, respectively. <sup>e</sup>  $P_p, P_i, P_g$  refer to the number of profile, intensity-dependent, and global refined parameters, respectively. Polycrystalline samples were sieved to 75 nm after very soft grinding and loosely deposited on a low-background crystal plate. The profile fitting of the data was performed with a pseudo-Voigt function, including asymmetry and preferred orientation corrections. Preferred orientation and asymmetry were corrected respectively by the March–Dollase and the Berar–Bardinozzi expressions (see ref 8).

The layered compounds  $\beta$ -MNX (M = Hf, Zr; X = Cl, Br) crystallize in the rhombohedral  $S\bar{m}SI$  structure type.<sup>9</sup> An individual layer consists of double sheets  $-X(MNNM)X-$ . Each metal atom is bonded to three halide (on the outside of the layer), three nitrogen (on the inside of the layer), and an additional nitrogen (from the second N sheet) that describe a capped trigonal antiprism. All atoms are located in 6c sites (0,0, $z$ ) with approximate  $z$  of 0.12, 0.20, and 0.39 for M, N, and X, respectively. As the space group and atomic positions

are preserved, the  $\beta$ -MNX compounds may be viewed as nitride intercalation derivatives from ZrCl rather than from the ZrBr stacking polytype structure.<sup>10</sup> The structure of the layered monohalides MX (M = Sc, Zr, Hf, Y, Ln and X = Cl, Br) consists of cubic close-packed layers of metal and halide atoms stacked in pairs, yielding the sequence X–M–M–X with relative orientations *AbcA*. They span metallic behavior from the physical and chemical points of view. The basic structure of the monohalide is preserved after oxidative chemical reactions providing  $M_2X_2Z_2$  or  $M_2X_2Z$  (M = Sc, Y, Ln; Z = H, C) and  $MXZ$  or  $MXZ_{0.5}$  (M = Zr, Hf; Z = H, C, O, N), where the nonmetal atoms (Z) occupy interstitial positions between the double metal layers.<sup>11–13</sup> In the zirconium halide derivatives, the anions  $O^{2-}$  (in  $ZrClO_{0.5}$ ),<sup>13</sup>  $C^{4-}$  (in  $ZrClC_{0.5}$ ),<sup>14</sup>  $H^-$  (in  $Zr_2X_2H$ ),<sup>15</sup> and  $N^{3-}$  (in  $\beta$ -ZrNX) (this work) occupy the tetrahedral sites. The insertion of the nonmetal atoms modifies the conduction band population. This determines the electronic properties, and often semiconducting, normal-valence compounds result. As in the alkaline-intercalated  $\beta$ -MNX compounds, superconductivity has been recently reported for the ternary lanthanide carbide halides  $Ln_2C_2X_2$  (Ln = La, Y, Lu; X = Br, I) as well as for their thorium-substituted or sodium-intercalated derivatives.<sup>16</sup> Between the structures of  $Ln_2C_2X_2$  and  $\beta$ -MNX families of compounds, common features and significant differences exist (See Figure 1b,c). The space group  $C2/m$  shown by the carbides is a subgroup of  $R3m$  and both structures exhibit the same topology for the metal-halide network. In contrast, the intercalated anions ( $C_2^{4-}$  and  $N^{3-}$ ) occupy octahedral intermetallic holes in the carbides and tetrahedral sites in the nitrides. As will be shown below, there are also significant differences in the corresponding electronic structures.

Chemical lithiation of  $\beta$ -ZrNCl,  $\beta$ -HfNCl, and  $\beta$ -ZrNBr with *n*-butyllithium leads to superconducting samples showing critical temperatures between 12 and 24 K. For both zirconium compounds, only one phase with ca. 0.2 lithium atoms per formula and  $T_c$  of 12 K (for ZrNCl) and 13.5 K (for ZrNBr) was found. Figure 4 shows the dependence of the magnetic susceptibility on temperature for the novel superconductor  $Li_{0.17}ZrNBr$ , as well as for  $Li_{0.20}ZrNCl$  and  $Li_{0.67}HfNCl$ . The superconducting transition for the bromide is 8 K wide, shows the onset at 13.5 K, and appears to indicate the existence of only one superconducting phase. ZFC measurements show a maximum 55% superconducting fraction, implying the existence of bulk superconductivity in the material. Lithiation of different  $\beta$ -HfNCl samples using the same experimental conditions lead to different lithium contents and critical temperatures. Bulk superconductivity was detected only for  $x \geq 0.17$ . Two different  $T_c$  were observed: 24 K for a sample with  $x = 0.67(3)$  (see Figure

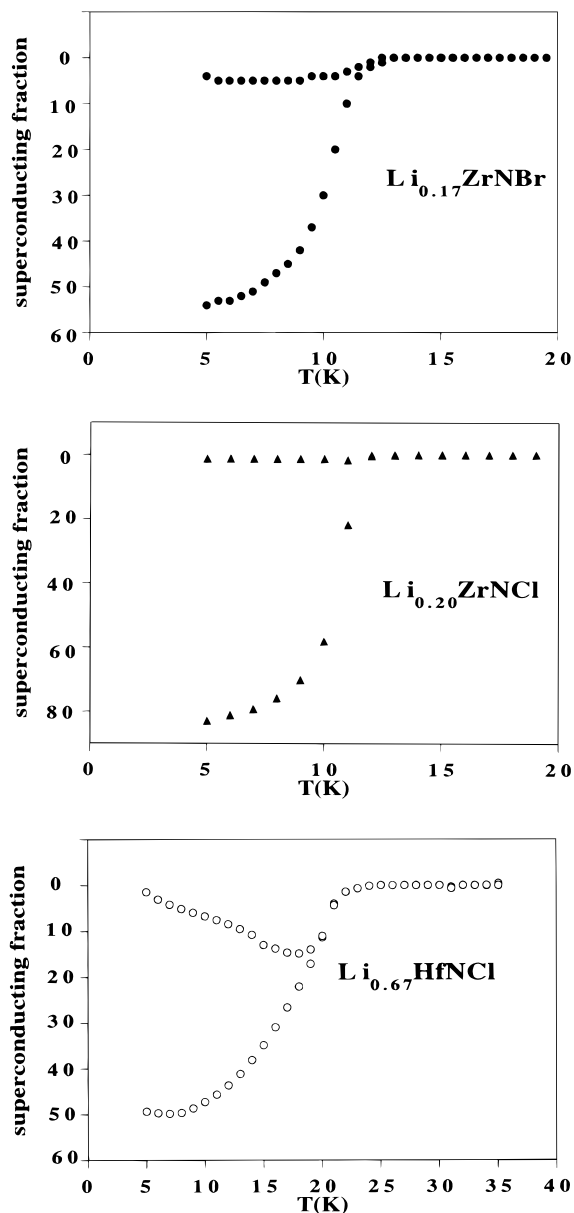


**Figure 4.** Magnetic susceptibilities for  $Li_{0.17}ZrNBr$ ,  $Li_{0.20}ZrNCl$  and  $Li_{0.67}HfNCl$ .

4), and 18 K for samples with a lithium content close to 0.4. This result significantly differs from that obtained by Yamanaka et al. in the lithiation of  $\beta$ -HfNCl with naphthyllithium in THF, where only a minimum change of  $T_c$ , between 25.5 and 24 K, was observed for a wide range of lithium contents.<sup>1</sup> According to the results obtained by chemical lithiation, Hf samples showed different electrochemical capacity for discharge, the larger corresponding to the samples with higher  $T_c$ . For different samples of the three host compounds,  $\beta$ -HfNCl,  $\beta$ -ZrNBr, and  $\beta$ -ZrNCl, two types of distinct electrochemical behavior were found. Whereas some samples show a plateau at around 1.8 V, as described in ref 17 for crystalline  $\beta$ -ZrNCl, other samples did not present this type of behavior and voltage decreased monotonically, as described for nonpurified  $\beta$ -ZrNCl.<sup>17</sup> However, in our case no impurities are seen in the X-ray diffrac-

(10) Ford, J. E.; Corbett, J. D.; Hwu, S. *Inorg. Chem.* **1983**, *22*, 2789–2790, and references therein.

(11) Corbett, J. D.; McCarley, R. E. *New Transition Metal Halides and Oxides*. In *Crystal Chemistry and Properties of Materials with Quasi-One-Dimensional Structures*; Rouxel, J., Ed.; Reidel Publishing: Dordrecht, 1986.

(12) Meyer, G.; Hwu, S.; Wijeyesekera, S.; Corbett, J. D. *Inorg. Chem.* **1986**, *25*, 4811.

(13) Seaverson, L. M.; Corbett, J. D. *Inorg. Chem.* **1983**, *22*, 3202.

(14) Ford, J.; Corbett, J. D.; Hwu, S. *Inorg. Chem.* **1983**, *22*, 2790.

(15) Wijeyesekera, S. D.; Corbett, J. D. *Inorg. Chem.* **1986**, *25*, 4709.

(16) Henn, R. W.; Schnelle, W.; Kremer, R. K.; Simon, A. *Phys. Rev. Lett.* **1996**, *77*, 374, and references therein.

(17) Ohashi, M.; Shigeta, T.; Yamanaka, S.; Hattori, M. *J. Electrochem. Soc.* **1989**, *136*, 1086–1089.

**Table 2. Exponents and Parameters Used in the Calculations**

atom	orbital	$H_{ij}$ (eV)	$\zeta_1$	$\zeta_2$	$c_1^a$	$c_2^a$
Zr	5s	-6.41	1.82			
	5p	-3.77	1.78			
	4d	-6.97	3.84	1.51	0.6210	0.5769
Hf	6s	-6.61	2.21			
	6p	-3.84	2.17			
	5d	-6.90	4.36	1.71	0.6967	0.5322
Y	5s	-6.01	1.74			
	5p	-3.62	1.70			
	4d	-5.74	1.56	3.55	0.8213	0.3003
Cl	3s	-26.64	2.18			
	3p	-14.22	1.73			
Br	4s	-25.21	2.59			
	4p	-12.96	2.13			
N	2s	-25.37	1.90			
	2p	-13.90	1.95			
C	2s	-19.65	1.63			
	2p	-11.13	1.63			

<sup>a</sup> Contraction coefficients used in the double- $\zeta$  expansion.

tion patterns of these samples. Further studies are in progress to elucidate these differences in behavior. It is clear, however, that no correlation exists between the presence of this plateau and the observation of superconducting properties in lithiated samples. On the other hand, electrochemical data are consistent with the results obtained from chemical lithiation, as the samples showing superconducting behavior are those showing higher electrochemical lithium uptake.

To gain some insight on the electronic structure of this material, we carried out tight-binding extended Hückel calculations<sup>18</sup> for  $\beta$ -ZrNCl (using our structure as well as that of Juza et al.),  $\beta$ -HfNCl,  $\beta$ -ZrNBr, and  $Y_2C_2Br_2$ . In the absence of crystal structures for the intercalated products, we have used a rigid band scheme to analyze the effect of lithiation. The main conclusions of our study are the following. First, the electronic structures of  $\beta$ -ZrNCl according to our crystal structure and that of Juza et al.<sup>4</sup> (see Figure 5a,b) are very different. This is especially true for the lower part of the d-block bands (i.e., the region above the energy gap) that is the region filled with the transferred electrons. Thus, in looking for correlations between  $T_c$  and the lithium content or structural details, it is essential to reason on the basis of the structure reported here. Second, as far as the region affected by the electron transfer is concerned, the electronic structures of  $\beta$ -ZrNCl and  $\beta$ -HfNCl are practically identical (compare parts a and c of Figure 5). In particular, the density of states at the Fermi level,  $N(e_f)$ , for a given number of transferred electrons is almost identical in both phases. Thus, assuming that the BCS theory is applicable, the higher  $T_c$  found for  $Li_{0.48}HfNCl$  ( $T_c = 25$  K) with respect to

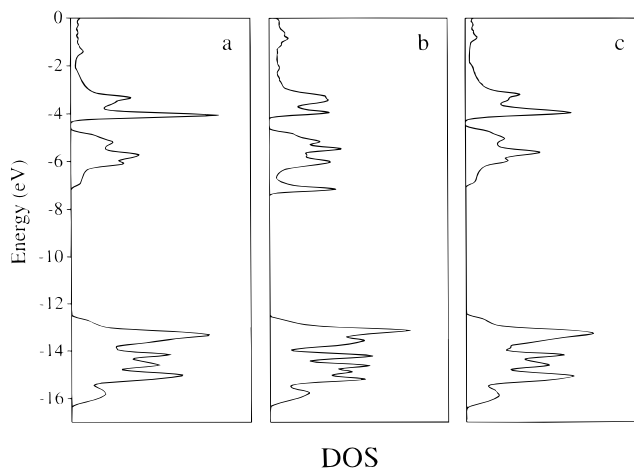


**Figure 5.** Calculated density of states (DOS) for (a)  $\beta$ -ZrNCl using our structure, (b)  $\beta$ -ZrNCl using the structure of Juza et al.<sup>5</sup> and (c)  $\beta$ -HfNCl. Upon lithiation the levels above the gap are filled.

$A_{\sim 0.48}ZrNCl$  ( $T_c = 15$  K) in the samples prepared by Yamanaka et al.<sup>1,2</sup> should not originate from differences in  $N(e_f)$  but from the existence of softer phonon modes in lithiated  $\beta$ -HfNCl. At this point it should be noted that the different  $x$  vs  $T_c$  dependencies found by Yamanaka et al.<sup>1</sup> and by us are really not that surprising. In our lithiated samples only lithium cations enter the van der Waals gap between the layers, occupying part of the holes and interacting strongly with the negatively charged halogen atoms. In the samples prepared with naphthyllithium-THF, solvent molecules are cointercalated so that, according to the model proposed,<sup>1</sup> most of the lithium cations do not interact directly with the halogen atoms but with the solvent. This means that for a given value of  $x$ , the phonon spectra of the layers must be more strongly affected in our samples than in those of Yamanaka et al. and the difference should increase with the value of  $x$ . Thus, different  $x$  vs  $T_c$  dependencies can be expected. Third, although phases such as  $\beta$ -HfNCl and  $Y_2C_2Br_2$  can be considered to belong to a common structural family, from the electronic point of view they are very different. For instance, whereas for any reasonable value of  $x$  in  $Li_xHfNCl$  the states near the Fermi level have mostly Hf character, those in  $Y_2C_2Br_2$  originate predominantly from the  $C_2^{4-}$  group. The topology of their band structures and Fermi surfaces are also very different. Thus, this type of lattice seems to provide for interesting variations on the electronic structure while the common structural features are kept and thus certainly deserve further attention.

**Acknowledgment.** This study was supported by the CICYT (grant MAT96-1037-C02), DGES (grant PB96-0859), and the Comissionat per Universitats i Recerca de la Generalitat de Catalunya (CIRIT, grants 1997-SGR24 and 1996-SGR51).

CM9810133

(18) Whangbo, M. H.; Hoffmann, R. *J. Am. Chem. Soc.* **1978**, *100*, 6093-6098. A modified Wolfsberg-Helmoz formula was used to calculate the nondiagonal  $H_{ij}$  matrix elements (Ammeter, J.; Bürgi, H. B.; Thibeault, J.; Hoffmann, R. *J. Am. Chem. Soc.* **1978**, *100*, 3686). The exponents, contraction coefficients, and atomic parameters are summarized in Table 2.